

Magnetization and Level Statistics at Quantum Hall Liquid-Insulator Transition in the Lattice Model

M. Niță¹ and A. Aldea²

¹*National Institute of Materials Physics, POBox MG7, Bucharest-Magurele, Romania*

²*Institut für Theoretische Physik, Universität zu Köln, D-50937 Köln, Germany*

Statistics of level spacing and magnetization are studied for the phase diagram of the integer quantum Hall effect in a 2D finite lattice model with Anderson disorder.

73.40.Hm,71.30.+h

The way in which the increasing disorder induces the insulating state when starting from the integer quantum Hall (IQH) state is a topic of controversy between the continuum and lattice models of the 2D electronic gas in strong magnetic field. The continuum approach predicts the crossover between the adjacent quantum Hall plateaus, ending up with the insulating state when the degree of disorder increases or, equivalently, the limit of small magnetic field is considered. This is due to the so-called 'floating up' of the critical energies E_c which occurs with increasing disorder. (E_c is the energy where the localization-delocalization transition takes place in the thermodynamic limit). In the critical region, i.e., when the Fermi energy E_f crosses an extended state energy E_c , the transverse (Hall) conductivity is $\sigma_{xy}^c = \nu - 1/2$ (at the transition between the plateaus ν and $\nu - 1$)¹. This means that at large disorder (or low field), the cascade of transitions must end with $\nu = 1 \rightarrow \nu = 0$ (insulator). The experiments give controversial information in what concerns the possibility to observe this last transition (see Ref.2 and the references therein, Ref.3) The sensible conclusion can be found in Ref.2 and Ref.4 suggesting that the theoretical results of the scaling theory, which are obtained for zero temperature and infinite systems, cannot be checked easily by experiments which are done for finite samples and at low (but nevertheless finite) temperature. The evaluation of the critical value of the longitudinal conductivity is also a difficult task. Lee, Kivelson and Zhang show in the frame of *corresponding states law* that $\sigma_{xx}^c = 1/2$ for any ν ; approaching the question in the opposite way, Zirnbauer assumes $\sigma_{xx}^c = 1/2$ and finds agreement with the numerical simulations. The numerical calculation performed by Huo, Hetzel and Bhatt for the lowest Landau level produces also 0.5; Huckestein and Backhaus show that this value is correct even in the presence of the electron-electron interaction⁵.

More recently, the same problem has been approached also in lattice models. The results are again controversial, since Yang and Bhatt⁶, in a discussion based on the calculation of the Chern numbers find a tiny floating-up of the extended states, while Xie et al⁷ do not find any changing in the position of extended states and affirm

that the floating picture is not valid in this model. The type of boundary conditions used in the lattice model is important; the above mentioned authors use periodic conditions. The Dirichlet conditions around the plaquette, which represent a more physical situation, are used by Sheng and Weng⁸; their approach, consisting in numerical calculation of the conductance performed over ensembles of disordered finite plaquettes, indicates that the QH-insulator transition may occur from any IQH plateau of index ν directly to the insulator. In the middle of the transition region the conductances satisfy the relation $\langle \sigma_{xx} \rangle = \langle \sigma_{xy} \rangle = \nu/2$ (here $\langle \dots \rangle$ means ensemble average) and the localization length diverges; this region is called 'metallic'.

In this context we study some new relevant features of the disordered lattice model in magnetic field with vanishing boundary conditions, the attention being paid especially to magnetization, level spacing distribution and critical conductances in the metallic region.

The discussion is based on the spin-less one-electron Hamiltonian in perpendicular magnetic field defined on a 2D square lattice with N sites in one direction and M sites along the other one, which reads as follows:

$$H = \sum_{n=1}^N \sum_{m=1}^M [\epsilon_{nm} |n, m\rangle \langle n, m| + i2\pi\phi m |n, m\rangle \langle n+1, m| + |n, m\rangle \langle n, m+1| + h.c.] \quad (1)$$

where $|n, m\rangle$ is a set of orthonormal states, localized at the sites (n, m) , and ϕ is the magnetic flux through the unit cell measured in quantum flux units. In Eq.(1) the hopping integral at $\phi = 0$ is taken unity serving as the energy unit and the diagonal energy ϵ_{nm} is a random variable distributed according to the probability density:

$$P(\epsilon) = \begin{cases} 1/W, & -W/2 < \epsilon < W/2 \\ 0, & otherwise, \end{cases} \quad (2)$$

(having zero mean $\bar{\epsilon} = 0$).

The averaged spectrum of Hamiltonian (1) is depicted in Fig.1 for $\phi = 1/10$ and the disorder amplitude in the range $W \in [0, 10]$. The lines represent the mean eigenvalues $\langle E_n \rangle$ as function of disorder amplitude W .

In order to study the phase diagram we calculate the longitudinal and Hall conductances of this system at constant magnetic flux and varying disorder. The different phases: quantum Hall, metallic, insulating are characterized not only by conductance but also by the specific

distribution of the level spacing and by the current density on the plaquette, described by the operator:

$$\mathbf{J}_{nm}^{n'm'} = i t_{nm}^{n'm'} (\mathbf{r}_{nm} - \mathbf{r}_{n'm'}) |nm\rangle\langle n'm'| + h.c \quad (4)$$

(here $t_{nm}^{n'm'}$ is the hopping integral between the sites \mathbf{r}_{nm} and $\mathbf{r}_{n'm'}$).

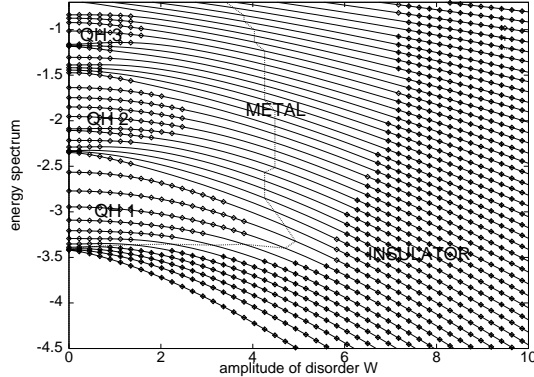


FIG. 1. Phase diagram of IQH effect. $N=M=10$. The insulator regime is depicted for $\sigma_{xx} < 0.2$ (in e^2/h units) and the metal regime for $\sigma_{xx} > 0.2$. In the QH regime $\sigma_{xy} = \text{integer}$ and σ_{xx} is negligible. The dotted line in the metallic region corresponds to the critical points ($\sigma_{xx} = \sigma_{xy}$).

It is opportune to remind previously that for a *clean* system ($\epsilon_{nm} = 0$) with cyclic boundary conditions (i.e for a torus) and commensurate values of the magnetic flux through the unit cell, the spectrum consists of degenerate bands separated by gaps (the well-known Hofstadter butterfly). However, when vanishing boundary conditions are imposed (i.e., for plaquette⁹ or cylinder¹⁰ geometry) the gaps get filled with 'edge states', localized close to the edges of the sample. The other states, the 'bulk' ones, remain grouped in bands on the energy scale, while geometrically are concentrated in the middle of the plaquette. The two types of states differ also by their chirality, i.e. by the sign of the derivative $dE_n/d\phi$.

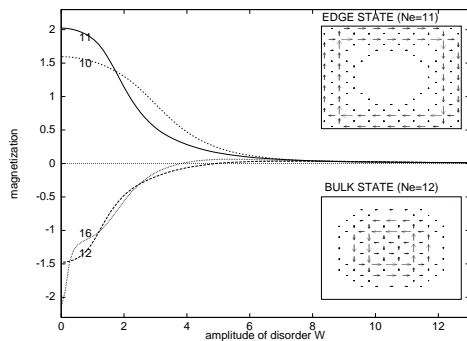


FIG. 2. The decay of the magnetization (in arbitrary units) with increasing disorder for the edge states No. 11 and 10 and for the bulk states No. 16 and 12. The distribution of current at $W = 0$ is shown in the insets. $\phi = 1/10$.

The effect on the orbital magnetization of each state is immediate: the expectation values of the operator $\mathbf{M} = \int (\mathbf{r} \times \mathbf{j}(\mathbf{r})) dS$ calculated on the eigenstates of

the Hamiltonian (1) have different signs depending on whether the state is bulk- or edge-type.

Fig.2 shows that the magnetization of the edge eigenstate No.11 is positive $M_{11} > 0$, but the bulk eigenstate No.12 has $M_{12} < 0$; the local currents corresponding to the two states are also shown in insets. In the same figure one anticipates that the increasing disorder produces a monotonic decrease of the magnetization. The magnetization of all states in the spectrum is shown in Fig.3a and b, for the clean and disordered system, respectively (the well-known electron-hole symmetry of the Hofstadter spectrum is evident also in the aspect of the magnetization). The disorder effect consisting in the broadening of the bands and narrowing of the gaps is obvious in the second figure. More notable is the magnetization of the ground state M_g which can be compared successfully with experimental results. Assuming that the spectrum is filled up to the Fermi energy E_f , due to the alternating sign of M_n in different regions of the spectrum, the quantity

$$M_g = \sum_{(E_n < E_f)} M_n \quad (5)$$

shows, as function of the number of occupied states, a sawtooth aspect (see Fig.4) which is the same as in the experiments by Wieggers et al¹¹, including the fact that the jumps of M_g occur at the center of the gaps. In our model, the number of teeth depends on the number of gaps that can be resolved. For modulated quantum wires such a sawtooth aspect was obtained also for the thermodynamic magnetization¹².

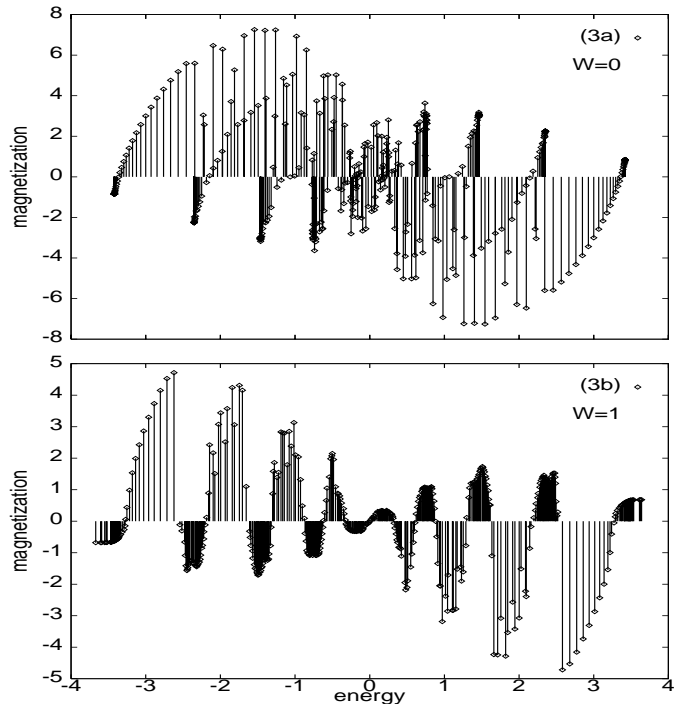


FIG. 3. Magnetization (in arbitrary units) vs. the energy. $W = 0$ in fig.3a and $W = 1$ in fig.3b. $N=M=20$. $\phi = 1/10$.

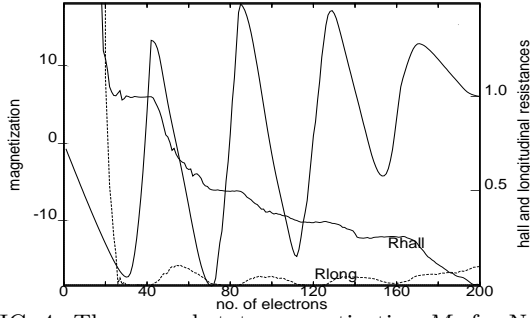


FIG. 4. The ground state magnetization M_g for $N=M=20$ and $W = 1$ vs. the number of electrons N_e (left scale). R_{xx} and R_{xy} for the same plaquette coupled to leads (right scale).

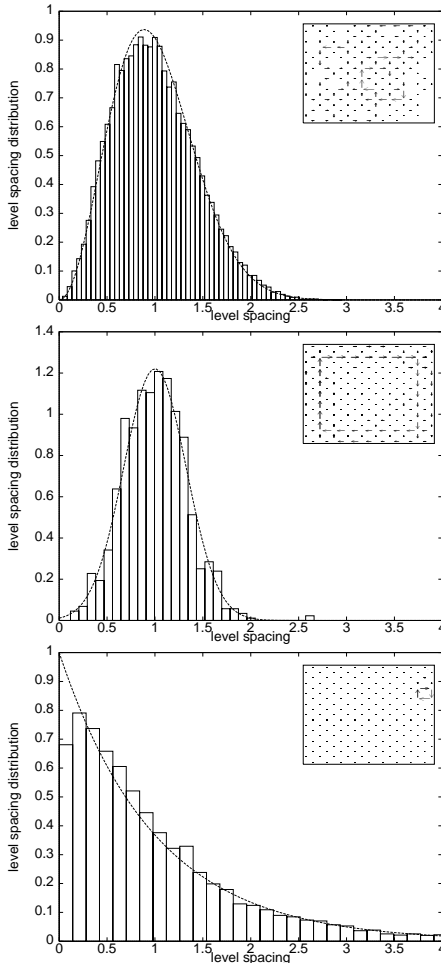


FIG. 5. Level spacing distribution $P(t)$ for three typical situations. Fig.5a gives the distribution of level spacing for $E \in [-2.4, -1.3]$ and $W = 3$. The dotted line is the Wigner-Dyson distribution with $\beta = 2$. In fig.5b $E \in [-2.9, -2.7]$ and $W = 1$. The dotted line is the Gaussian function whose variance equals the calculated variance of the histogram $\delta(t) = 0.33$. In fig.5c $E \in [-8, -6]$, $W = 13$ and $\delta(t) = 0.92$. The dotted line is the Poisson function. The corresponding typical current distributions are shown in the insets. $N=M=10$ and the number of disorder configurations is equal to 1000. $\phi = 1/10$.

When the Anderson potential (Eq.2) is switched on and W is increased continuously, the bands become broader and broader, the disorder spreads the states over the whole plaquette, giving rise to extended disordered states, and finally produces a quasi-continuum of localized states; even the edge states, which are more robust, disappear gradually into the quasi-continuum. The nature of the states can be checked by calculating the distribution of level spacing for various degrees of disorder, in different domains of the spectrum. Let s_n be the level spacing between two consecutive eigenvalues E_n and E_{n+1} and define $t_n = s_n / \langle s_n \rangle$, where $\langle s_n \rangle$ is the mean level spacing.

In Fig.5 we have three typical distribution functions $P(t)$ relevant for different values of disorder and energy interval. The Wigner-Dyson (WD) surmise with $\beta = 2$ (unitary) indicates the presence of extended states (Fig.5a) and the Poisson-like distribution (Fig.5c) shows the existence of uncorrelated localized states for strong disorder. The case of edge states is also studied, in which situation the distribution can be fitted well with the Gaussian function (Fig.5b). Every inset shows a representative distribution of local currents for each case. Very illustrative is Fig.6 which shows the variance δt_n for all level spacing of the Hamiltonian (1). One may learn that: a) at $W < 4$, for most of the states, $\delta t_n \approx 0.42$, which is the typical value for WD distribution with $\beta = 2$. b) for larger W , the variance increases towards $\delta t_n = 1.0$ specific to the Poisson distribution. This value cannot practically be reached because of finite dimension of the plaquette. c) inbetween, at $W \approx 6$, the variance equals 0.52, and the probability distribution is well-fitted by the WD function with $\beta = 1$ (so, here the influence of the magnetic field is lost and the system behaves 'orthogonal'). d) the lowest states, originating from the first band ($n=1, \dots, 6$) get localized faster than the others, while the states from the first gap ($n=7, \dots, 10$) are very robust against the localization process.

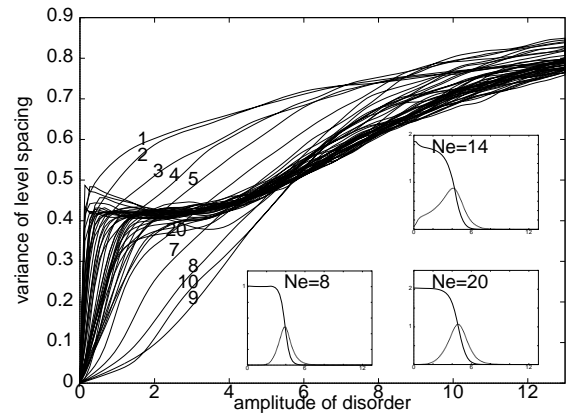


FIG. 6. The variance of level spacing $\delta(t_n)$ ($n=1, \dots, 50$) vs. amplitude of disorder W . $N=M=10$. The insets show the evolution of σ_{xx} and σ_{xy} at a given number of electrons N_e vs. W (for the same plaquette coupled to semiinfinite leads).

At last we discuss the transport properties; for this purpose the Landauer-Büttiker formalism and the techniques from Ref.9 are used. The conductance in the three regimes (IQH, metal and insulator) may be correlated with the spectrum characteristics of the isolated system discussed above. Since the edge states are responsible for IQH effect and they are robust against disorder, this regime survives also in the presence of disorder as long as W is not too high. In what concerns the transmitances between different leads, it is well-known that the only non-vanishing ones are $\langle T_{\alpha\alpha+1} \rangle$, which connect consecutive leads (α =lead index) and equal an integer value.

The metallic regime occurs when the transport process takes place on the states which are extended over the whole plaquette. In this case also the local current is distributed on the whole area allowing for a non-zero transmission probability between any pair of leads. This behaviour corroborates with the multi-fractal properties of the local density of states¹³. The metallic region can be crossed in different ways. Let assume a constant disorder (say $W = 1.0$) and change the Fermi level; in this case, metallic regions are intercalated between the QH regions, excepting the lowest one which ensures the transition between QH1 and the insulating phase. The consequence is that, when crossing the metallic region, the Hall conductance σ_{xy} will have a smooth decay between consecutive plateaus, while σ_{xx} will differ from zero and have a maximum in the middle of the transition. In Fig.4, one has to notice that R_{xx} equals R_{xy} in two places: 1) at the transition between QH1 and insulator, where one has also $\sigma_{xx} \approx 1/2$ in agreement with Huo at al⁵, and 2) near the centre of the spectrum where the system behaves already classically.

Another way to look at the metal-insulator transition consists in crossing the metallic zone by increasing the amplitude of disorder W , while keeping constant the number of electrons (N_e) or the Fermi level. Now the transition is of the type $\nu \rightarrow 0$ and exhibits maxima of the longitudinal conductance at a critical disorder W_c where, as in Ref.8, the condition $\sigma_{xx} = \sigma_{xy}$ is fulfilled. Such kind of transitions are shown in the insets of Fig.6 for $N_e=8$ (i.e. in the first gap) and for $N_e=20$ (i.e. in the second gap). One may ask what is going on when N_e corresponds to a band; this is the situation for the third inset $N_e=14$. It can be observed that σ_{xx} is different from zero even at small W , meaning that the bulk states are the first ones which become extended under the influence of disorder. The dotted line which crosses transversally the spectrum in the metallic region of Fig.1 represents the critical disorder W_c corresponding to each N_e .

In the insulating phase, when the Poisson distribution of the level spacing is installed, the Hall and longitudinal conductances tend to zero and the longitudinal resistance increases exponentially. The transport of the electron through the plaquette is performed by tunneling on localized states.

In conclusion, the metallic regime is characterized by a Wigner-Dyson distribution of the level spacing with $\beta = 2$ (unitary ensemble). As the system evolves towards insulator, the orthogonal WD distribution ($\beta = 1$) that shows up at a given higher disorder indicates the loss of influence of the magnetic field. Simultaneously, the magnetization decays to zero. The QH phase is characterized by a Gaussian distribution of level spacing. Due to the different chirality of the edge and extended states, when crossing the metallic zone (at relatively small disorder) the magnetization of the ground state shows a tooth saw behavior as function of the filling factor similar to experimental results.

Acknowledgments. A.A. is very grateful to Professor Johannes Zittartz for his hospitality at Institut für Theoretische Physik der Universität Köln where this work was partially performed under SFB 341. Illuminating discussions with J.Hajdu, B.Huckestein, M.Zirnbauer, K.Maschke and A.Manolescu are thankfully acknowledged. We thank Romanian Academy for the support under the grant No.69/1999.

*Permanent address: National Institute of Materials Physics POBox MG7, Bucharest-Magurele, Romania.

-
- ¹ D. E. Khmel'nitskii, Phys. Lett. **106A**, 182 (1984); B. Laughlin, Phys. Rev.Lett.**52**,2304(1984); S. Kivelson, D. H. Lee and S.C.Zhang, Phys.Rev.B **46**, 2223 (1992).
 - ² S.Das Sarma in *Perspectives in Quantum Hall Effects*, edited by S.Das Sarma and Aron Pinczuk, John Wiley & Sons,Inc., New York, 1997;
 - ³ M.Hilke,D.Shahar,S.H.Song,D.C.Tsui and H.Xie, preprint cond-mat/9906212.
 - ⁴ B.Huckestein, Phys.Rev.Lett. **84**,3141 (2000)
 - ⁵ D.H.Lee, S.Kivelson and S.C.Zhang, Phys. Rev. Lett. **68**, 2386 (1992); M.R.Zirnbauer, preprint cond-mat/9905054; Y.Huo,R.E.Hetzel,and R.N.Bhatt, Phys. Rev. Lett. **70**, 481 (1993); B. Huckestein and M. Backhaus, Phys. Rev. Lett. **82**, 5100 (1999).
 - ⁶ K.Yang and R.N.Bhatt, Phys.Rev.Lett. **76**,1316(1996); K.Yang and R.N.Bhatt, Phys.Rev.B **59**,8144 (1999).
 - ⁷ D.Z.Liu,X.C.Xie and Q.Niu, Phys. Rev. Lett. **76**, 975 (1966); X.C.Xie,D.Z.Liu,B.Sundaram and Q.Niu, Phys. Rev. B**54**, 4966 (1966).
 - ⁸ D.N.Sheng and Z.Y.Weng, Phys.Rev.Lett. **80**,580(1998).
 - ⁹ A.Aldea,P.Gartner,A.Manolescu and M.Niță, Phys.Rev. B **55**, R13389(1997). F.Gagel and K.Maschke, Phys.Rev.B **52**,2013 (1995).
 - ¹⁰ C.Schulze,J.Hajdu,B.Huckestein,and M.Janssen, Z.Phys.B 103,441 (1997).
 - ¹¹ S.A.J.Wiegers,M.Specht,L.P.Levy,M.Y.Simmons, D.A.Ritchie,A.Cavanna,B.Etienne,G.Martinez and P.Wyder, Phys.Rev.Lett.**79**,3238 (1997).
 - ¹² S.I.Erlingsson,A.Manolescu and V.Gudmunsson, Physica E,**6**,763 (2000).
 - ¹³ M.Janssen,M.Metzler,M.R.Zirnbauer, Phys.Rev.B **59**, 15836 (1999).